Histol Histopathol (2024) 39: 165-175

Histology and Histopathology
From Cell Biology to Tissue Engineering

ORIGINAL ARTICLE Open Access

Calpain-specific breakdown fragment in human drusen

Kana Orihara[1], Momoko Kobayashi-Otsugu[1], Emi Nakajima[1,3], Ryan D. Walkup[1,3], David J. Wilson[2], Thomas R. Shearer[3] and Mitsuyoshi Azuma[1,3]

[1]Senju Laboratory of Ocular Sciences, Senju Pharmaceutical Corporation Ltd., [2]Department of Ophthalmology, School of Medicine and [3]Department of Oral Rehabilitation and Biosciences, Oregon Health and Science University, Portland, OR, USA

Summary. Purpose. With aging and age-related macular dystrophy (AMD), proteolytic fragments are deposited in extracellular drusen located between the RPE and Bruch's membrane. Localized hypoxia may be a risk factor for AMD. Our hypothesis is that following hypoxia, activation of proteolytic enzymes called calpains may cause proteolysis/degeneration of retinal cells and RPE. No direct evidence has yet demonstrated activation of calpains in AMD. The purpose of the present study was to identify calpain-cleaved proteins in drusen.

Methods. Seventy-six (76) drusen were analyzed in human eye sections from six normal and twelve AMD human donor eyes. The sections were subjected to immunofluorescence for the calpain-specific 150 kDa breakdown product from α-spectrin, SBDP150-a marker for calpain activation, and for recoverin-a marker for photoreceptor cells.

Results. Among 29 nodular drusen, 80% from normal eyes and 90% from AMD eyes stained positive for SBDP150. Among 47 soft drusen, mostly from AMD eyes, 72% stained positive for SBDP150. Thus, the majority of both soft and nodular drusen from AMD donors contained SBDP150.

Conclusions. SBDP150 was detected for the first time in soft and nodular drusen from human donors. Our results suggest that calpain-induced proteolysis participates in the degeneration of photoreceptors and/or RPE cells during aging and AMD. Calpain inhibitors may ameliorate AMD progression.

Key words: Calpain, α-spectrin, SBDP150, AMD age-related macular degeneration, Drusen

Corresponding Author: Mitsuyoshi Azuma, Director, Senju Laboratory of Ocular Sciences, Senju Pharmaceutical Corporation Ltd., Portland, OR, 97239, USA. e-mail: azumam@ohsu.edu
www.hh.um.es. DOI: 10.14670/HH-18-635

Introduction

Terminology

"Nodular drusen" are small hard drusen. "Soft drusen" are larger clustered deposits showing indistinct borders. The "macula" exhibits multiple ganglion cell layers, while "mid periphery" is the outer portion exhibiting only single layer of ganglion cells (Fig. 1). Different drusen types co-exist at certain locations in retina (Azuma et al., 2010; Yang et al., 2016).

Drusen in AMD

Aged-related macular degeneration (AMD) is a leading cause of vision loss in the elderly. AMD is characterized by the loss of retinal pigment epithelium (RPE) and photoreceptor layers. Accumulation of yellowish, insoluble extracellular deposits (drusen) occurs between the basal lamina of RPE and the inner collagenous layer of Bruch's membrane (BrM). Drusen are known to contain components derived from RPE cells, blood proteins, immune-associated elements, proteins related to lipids and the extracellular matrix underlying Bruch's membrane, and mineralized hydroxylated calcium phosphate stabilized by vitronectin (Chakravarthy et al., 2010; Fernandez-Godino et al. 2016, Shin et al., 2020; Spaide et al., 2020).

Early dry (non-exudative) AMD shows small drusen that may not affect vision. Late AMD is characterized by sharply delineated areas of degenerated RPE cells, and visible choroidal vessels (Azuma et al., 2010; Yang et al., 2016). Late advanced AMD can be non-exudative or exudative. Exudative AMD involves the exudation or leakage of fluid and blood from new blood vessels. Exudative AMD shows atrophy of the outer retina, thinning and loss of the RPE, and neovascular AMD. Neovascularization beneath the macula may cause fluid swelling often leading to permanent loss of central vision (Spaide et al., 2020). The mechanisms proposed include VEGF secretion by stressed RPE, macrophage

activity during breaching of BrM, invading capillaries that remove or replace friable deposits, and damage to surrounding cells by peroxidized lipids (Curcio et al., 2018b).

Mechanism of AMD

Loss of the RPE is pathogenic in AMD because RPE normally phagocytose shedding photoreceptor outer segments to remove photooxidative products and maintain photoreceptor excitability. Further, RPE cells cause degranulation or shedding of granule aggregates resulting in decreased autofluorescence (Gambril et al., 2019). Disturbances of choroidal blood flow, choroidal ischemia, and drusen accumulation with decreased choroidal blood volume have been reported in AMD eyes (Tisi et al., 2021). Thus, hypoxia-mediated changes to photoreceptor and/or RPE cells have been implicated as one of the factors causing AMD (Curcio, 2018b; Spaide et al., 2020).

A consequence of hypoxia in the outer retinal layers is activation of a superfamily of calcium-dependent, cysteine proteases called calpains (Ono and Sorimachi., 2012). In our previous studies, photoreceptor and RPE cells cultured under hypoxia showed activation of calpains, proteolysis of substrates (e.g., α-spectrin), and cell death (Nakajima et al., 2017). Calpain activation and proteolysis of various molecules also mediate irreversible Ca^{2+} signaling and initiate cell death mechanisms. For example, breakdown of the scaffold protein α-spectrin by calpain resulted in loss of cytoskeletal integrity during cell death (Hirata et al., 2015; Nakajima et al., 2017).

Our hypothesis is that aging and hypoxia cause loss of RPE cell integrity, increase intracellular calcium, and activate calpain. Calpain proteolysis of cytoskeletal proteins α-spectrin, vimentin and vitronectin occurs in the photoreceptor cells and/or RPE cells. RPE cells normally phagocytose shed photoreceptor outer segments. Phagocytosis by RPE would lead to accumulation of calpain-damaged proteins in the RPE. Dysregulated phagocytosis caused by stressed, overburdened RPE may then result in accumulation of calpain-cleaved material in drusen. A limited study (Lambert et al., 2016) has already detected cytoskeletal proteins in drusen.

Drusen are thus early bio-markers for AMD. The purpose of the present study was to detect calpain-proteolyzed protein in drusen. Finding calpain-proteolyzed protein in drusen suggests that treating AMD patients with a calpain inhibitor drug would ameliorate cytoskeletal protein degradation, protect neuronal cells (Nakajima et al., 2011), and protect against RPE cell death (Nakajima et al., 2017).

Materials and methods

Eye tissues

Human eyes were obtained from the Lions VisionGift (Portland, OR, USA), using informed consent that was exempt from IRB review. We analyzed 29 nodular drusen and 47 soft drusen from 22 AMD donors categorized by the eye bank. All eyes were kept at 4°C and processed 5-24 hours postmortem. The 4°C holding temperature attempted to ameliorate hypoxia and postmortem activation of calpain. Thus, postmortem activation of calpain in human donor eyes was possible, but not controllable due to protocols at the eye bank. Our research complied with the tenets of the Declaration of Helsinki for Ethical Principles for Medical Research Involving Human Subjects.

SBDP150 immunoblotting

Proteins from RPE, drusen and choroid were isolated together from the donor eyes. Eyes from an 87-year old male donor were frozen in liquid nitrogen and stored at -80°C. Eyes were thawed for half a day at 4°C on ice; the anterior segment, vitreous and optic nerve

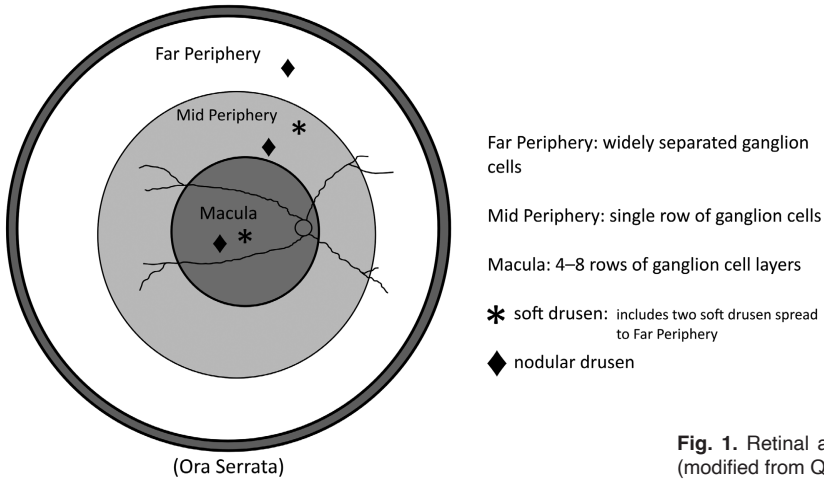

Fig. 1. Retinal areas surveyed. Illustration of the different retinal regions (modified from Quinn et al., 2019) and the types of drusen found.

were removed. The eye cups were dissected into six fan-shaped petals (>5 mm) in HBSS (Corning, Glendale, AZ, USA). To collect proteins from the high-risk drusen area, the petal containing the macula was identified and used. After slowly separating the retina, RPE with drusen and choroid were isolated from the interior surface.

Samples were collected in RIPA buffer (Thermo Fisher Scientific, Waltham, MA, USA) with protease inhibitors (Complete Mini-EDTA-free, MilliporeSigma, Burlington, MA, USA), sonicated and centrifuged. Three µg lysate per lane were electrophoresed in 4-12% NuPAGE gels with MOPS buffer (Thermo Fisher Scientific) at 175 V for 120 minutes on ice. Proteins were then electrotransferred to polyvinylidene difluoride (PVDF) membranes at 100 V for 90 minutes. Transferred membranes were blocked with 5% skim milk in Tris-buffered saline containing 0.05% Tween 20 (Bio-Rad Laboratories, CA, USA). Blocked membranes were then incubated at 4°C overnight with a 1:1000 dilution of custom made SBDP150 antibody (rabbit monoclonal, Senju Pharmaceutical, Co., Ltd., Kobe, Japan) produced by hybridoma cells against the N-terminal six amino acids (GMMPRC) at the cleavage site on the calpain-specific α-spectrin breakdown product at 150 kDa (SBDP 150 kDa) (Hirata et al., 2015). Protein bands were visualized with a secondary antibody against rabbit IgG conjugated to horseradish peroxidase enzyme (incubated at 1:3000) (Santa Cruz Biotechnology, Dallas, TX, USA) and ECL Prime Western Blotting Detection Reagent (Cytiva, Marlborough, MA, USA). Images of the stained membranes were captured with FluorChem FC2 imager (ProteinSimple, San Jose, CA, USA). For neutralization of the SBDP150 antibody, excess amounts of antigenic peptide were incubated with SBDP150 antibody at 4°C for several days. Neutralized antibody was then used in place of the primary antibody.

Immunofluorescence

Whole eye globes were fixed in 10% formalin, embedded in paraffin, and the whole eyecup was sliced at five µm. Formalin-fixed paraffin sections were incubated for immunofluorescence with antibodies against SBDP150 described above (1:50 dilution). Recoverin, a cytoplasmic marker for photoreceptor cells (Hendrickson et al., 2008; MilliporeSigma, 1:20) was incubated overnight at 4°C. After washing three times with PBS, the sections were incubated with secondary antibodies against rabbit IgG conjugated to Alexa Fluor 568 for SBDP150 and against mouse IgG conjugated to Alexa Fluor 488 for recoverin (1:200 each; Thermo Fisher Scientific), together with Hoechst 33342 dye (1:500 dilution; Thermo Fisher Scientific) for visualization of nuclei. Anti-SBDP150 neutralized with excess antigen peptide or non-immunized IgG were used as negative staining controls. Slides were mounted in ProLong Gold anti-fade solution (Thermo Fisher Scientific) with cover slips. Photomicrographs were imaged with a fluorescence microscope and captured with a digital camera (Axio Observer 7 microscope and AxioCam MRm camera, Carl Zeiss, Oberkochen, Germany) with an ECPlan-Neofluar 20x objective (air, aperture 0.50). Images were compiled using ImageJ 1.53c (http://imagej.nih.gov/ij/; provided in the public domain by National Institutes of Health, Bethesda, MD, USA). Staining of drusen was performed on the posterior portion of each section containing retina, RPE/choroid, and sclera.

H&E staining

Paraffin-embedded tissues sections (5 µm) were stained with hematoxylin (Epic Scientific, San Diego, CA, USA) for 5 minutes and with eosin (Fisher Scientific) for 45 seconds. The tissue sections were examined under a light microscope (Zeiss Primovert and Axiocam 105) after mounting with Acrymount mounting medium (StatLab, McKinney, TX, USA).

Results

Immunoblotting

A single band, migrating at the expected 150 kDa position for the calpain-specific cleavage site on α-spectrin, was observed in the dissected RPE/choroid/drusen sample (Fig. 2A, SBDP150, lane 1) and in the whole retina sample (Fig. 2B). The specificity and identity of this band were confirmed by loss of the 150 kDa band when the SBDP150 antibody was neutralized with excess SBDP150 antigenic peptide (Fig. 2A,B, SBDP150, lane 2).

Histological sections from normal and AMD-affected human retina were first examined for drusen (Fig. 2C). Table columns labeled “Number observed” show drusen totals within each AMD diagnosis. Nodular drusen were observed in macula, and both in mid and far peripheral areas. Soft drusen were found in macula and mid periphery. As expected, more drusen were observed in AMD patients (3.0 drusen per eye) than in the normal group (1.1 drusen per eye).

Frequency of SBDP150 in human drusen

The seventy-six nodular and soft drusen above from 8 normal eyes (4 donors), and 22 AMD eyes (12 donors, various types) were stained for SBDP150. Overall, 57 drusen (75%) were positive for SBDP150 (Fig. 2C, Table 1). Results varied somewhat due to the cut angle of the single histological section from each eye.

Detailed localization of SBDP150 in nodular drusen

Bright field images showed small, hard nodular drusen between the RPE-BL and inner collagenous layer of BrM (Fig. 3A). Immunofluorescence showed a strong

red signal for SBDP150 in nodular drusen (Fig. 3B).

The sections were also counter stained for cell nuclei DNA with Hoechst 33342 (blue, Fig. 3C). Nuclei were found in the choroid below BrM, but not in nodular drusen. Also, loss of the single layer of healthy RPE cells in this area was observed, suggesting that RPE cells were degenerated. Negative IgG control slides showed lack of SBDP150 staining in the nodular drusen (Fig. 3D). However, autofluorescence of the RPE was always present (yellow arrow heads, Fig. 3B,D). The autofluorescence of the RPE cells is attributed to the accumulation of lipofuscin and melanolipofuscin (Bermond et al., 2021), since RPE showed fluorescence even when normal IgG was used in place of the antibody. When RPE marker, RPE65 was used, the RPE layer sometimes showed brighter fluorescence. But it

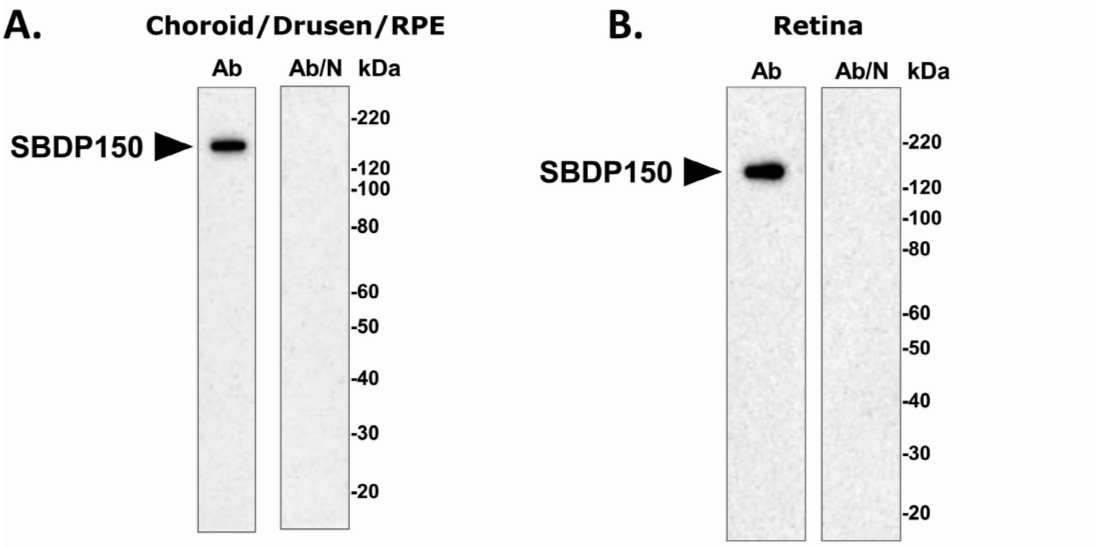

C. Frequency of SBDP150-positive drusen in regions of retina

	Nodular Drusen in Mid and Far Periphery			Nodular Drusen in Macula		
Patient Diagnosis (eyes)	Number observed (n)	Number SBDP150-positive (n)	**Frequency SBDP150-positive (%)**	Number observed (n)	Number SBDP150-positive (n)	**Frequency SBDP150-positive (%)**
Normal (8)	5	4	**80**	0	0	**0**
Dry AMD (9)	7	6	**86**	1	1	**100**
Wet AMD (3)	3	3	**100**	2	1	**50**
Mixed AMD (4)	4	3	**75**	0	0	**0**
AMD/Glaucoma (6)	5	5	**100**	2	0	**0**

	Soft Drusen in Mid Periphery			Soft Drusen in Macula		
Patient Diagnosis (eyes)	Number observed (n)	Number SBDP150-positive (n)	**Frequency SBDP150-positive (%)**	Number observed (n)	Number SBDP150-positive (n)	**Frequency SBDP150-positive (%)**
Normal (8)	2	1	**50**	2	0	**0**
Dry AMD (9)	9	7	**78**	9	7*	**78**
Wet AMD (3)	3	3	**100**	3	2	**67**
Mixed AMD (4)	3	1	**67**	4	3	**75**
AMD/Glaucoma (6)	6	4	**67**	6	5	**83**

Fig. 2. Immunostaining of SBDP150 in various types of drusen. **A.** Immunoblot using SBDP150 antibody on proteins from a dissected human retina containing choroid, RPE layers and drusen. The blot showed the expected 150 kDa band for calpain-induced spectrin breakdown fragment (Ab,1st lane, left). The band was absent when the extracts were immunostained with SBDP150 antibody previously neutralized with excess immunizing peptide (Ab/N, 2nd lane), confirming specificity of antibody. MW markers in kDa (3rd lane). **B.** Immunoblot of proteins extracted from total human retina immunostained with SBDP150 antibody, showing the SBDP150 band (Ab, 1st lane, left). This band was absent in extracts immunostained with neutralized SBDP150 antibody (Ab/N, 2nd lane), MW markers in kDa (3rd lane). **C.** Number of donors and types of drusen in macula, mid and far peripheral regions identified by SBDP150 antibody in (A). Eight (8) eyes from 4 normal donors, and 22 eyes from 12 donors with various types of AMD allowed examination of 76 drusen of which 57 (75%) were positive for SBDP150. Type of AMD was indicated on the Eye Bank donor information sheet. Example in shaded box reads: "In a total of 8 eyes from the mid and far peripheral retinas of normal patients, 5 nodular drusen were observed, and 4 (80%) were positive for SBDP150." *One eye contained a nodular druse positive for SBDP150 in dry AMD and also a soft druse positive for SBDP150.

was still difficult to determine if RPE65 proteins were present in drusen due to high RPE autofluorescence. When neutralized SBDP150 antibody was used, the staining of SBDP150 was blocked in the nodular drusen (Fig. 3E). These facts also confirm that nodular drusen contain SBDP150.

Nodular drusen were also immunostained with an antibody against recoverin, a cytoplasmic marker for photoreceptor cells that can detect both rods and cones (green, Fig. 3F) (Hendrickson et al., 2008). Counterstaining was used with Hoechst 33342 (blue, Fig. 3G). Recoverin antibody specificity was confirmed by the western blot in Fig. 4. Although recoverin staining was weak, we confirmed recoverin location in the same area as for SBDP150 in nodular drusen. The negative IgG control slide showed lack of recoverin staining in nodular drusen (Fig. 3H). When neutralized recoverin antibody was used, the staining of recoverin was also blocked in nodular drusen (Fig. 3I). Nodular drusen, including those not stained with SBDP150, were most frequently observed in the mid periphery and far periphery from normal and AMD donors. The percentage of the 23 nodular drusen in mid periphery and far periphery that stained positive for SBDP150 was nearly the same in normal (80%) and AMD (89.5%) donors (Fig. 3J, Table 1). Additionally, in a total of 29 nodular drusen, 47.8% were positive for both recoverin and SBDP150 (Table 1). Thus, both recoverin and SBDP150 are part of the components of nodular drusen.

Detailed localization of SPDP150 in soft drusen

Soft drusen are defined as partially preserved lipoprotein build-up on the BrM (Curcio, 2018a). Bright field imaging located an upper area occupied by rod outer segments (ROS), RPE (upper dark layer), and the BrM (lower membrane) (Fig. 5A). These areas were separated by a large intervening area of soft drusen. Immunofluorescence with the SBDP150 antibody showed SBDP150 in the soft drusen from a dry AMD donor (Fig. 5A-I) and a wet AMD donor (Fig. 6A-D).

A limitation of our study is the small number of drusen samples. Also, we were not able to adequately resolve the precise location of the positive SBDP150 staining below the RPE in the basal laminar deposit (BLamD). Thickening at this location is considered as an important sign of AMD progression (Sura et al., 2020). Further study with TEM would clarify if SBDP is present.

Counter staining with Hoechst 33342 cell nuclei marker (blue) showed photoreceptors and outer blood vessel cells that were not detected in soft drusen (Fig. 5C). Also, instead of a healthy single layer of RPE cells, loss of nuclei was observed in the RPE layer, suggesting

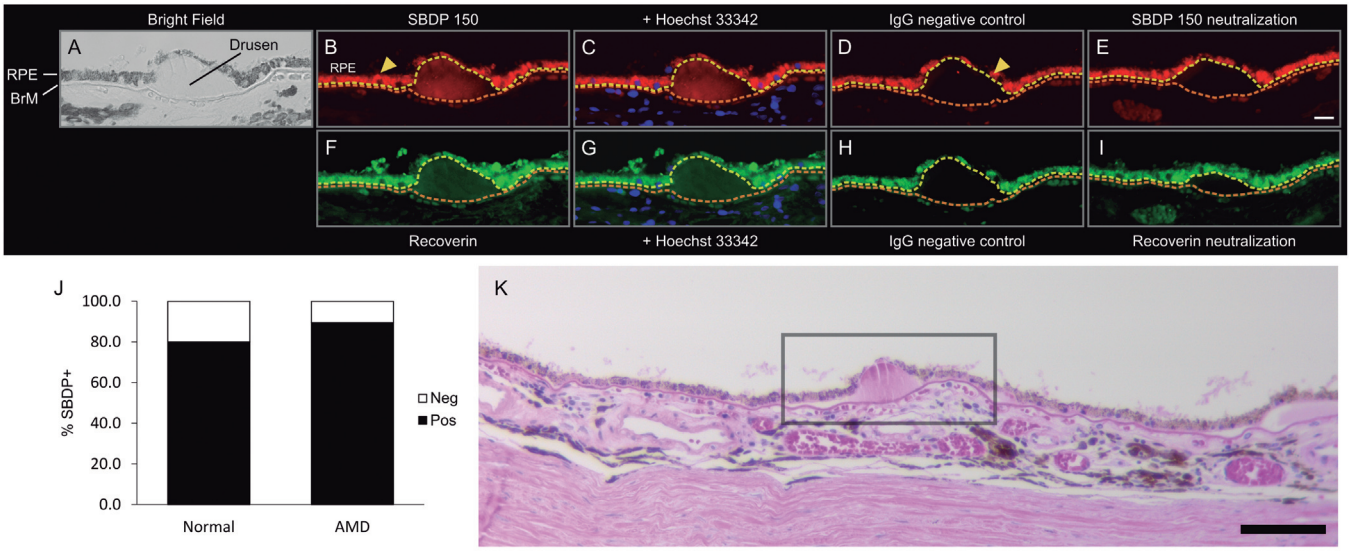

Fig. 3. Immunofluorescence performed on nodular drusen in far periphery from a 77-year-old female donor with dry AMD showing localization of SBDP150, photoreceptor proteins, and appropriate staining controls. **A.** Bright field image of nodular drusen, followed by four consecutive sections for: **B.** SBDP150 localization (red) in drusen. Bruch's membrane (lined with the orange dotted line) and RPE (above the yellow dotted line) were identified. **C.** Counter staining with Hoechst 33342 stain for DNA from cell nuclei (blue), which were found in the RPE layer and in the choroid below Bruch's membrane, but not in drusen. **D.** Negative IgG control slide showing no SBDP150 staining. However, autofluorescence of the RPE was always present (yellow arrow head). **E.** Additional negative control showing loss of SBDP150 staining in nodular drusen when the slide was treated with neutralized SBDP150 antibody. **F, G.** In place of SBDP150 antibody, nodular drusen in this section were processed with an antibody against the photoreceptor protein recoverin, showing positive staining (green) and counterstaining with Hoechst 33342 (blue, G). Note similar localization of recoverin as with SBDP150 in nodular drusen. **H.** Negative IgG control slide showing no recoverin staining. **I.** Loss of recoverin staining occurred when the slide was treated with neutralized recoverin antibody. **J.** The percentage of nodular drusen staining positive for SBDP150 was similar in normal (80%, n=5) and AMD donors (89.5%, n=19). **K.** H&E staining with boxed area showing nodular druse 10x. Scale bars: A-I, 20 μm; K, 100 μm.

that RPE cells were degenerated during AMD development. As expected, the negative IgG control and peptide neutralization slides showed lack of SBDP150 staining in the soft drusen (Fig. 5D,E). Autofluorescence of the RPE is indicated with yellow arrow heads (Fig. 5B,D).

Soft drusen along with photoreceptors were also weakly immunostained with recoverin antibody (green, Fig. 5F, 4 consecutive sections). Counter-staining was used with Hoechst 33342 (blue, Fig. 5G). The results showed recoverin and SBDP150 existed in the same area in soft drusen. Negative IgG control slide showed lack of recoverin staining in the soft drusen (Fig. 5H). When neutralized recoverin antibody was used, the staining of recoverin was blocked in the soft drusen (Fig. 5I). The results showed similar locations for recoverin and SBDP150 in soft drusen, as seen in nodular drusen. Soft drusen were observed in both macula and the mid peripheral areas from AMD donors. The percentage of soft drusen in AMD donors that stained positive for SBDP150 was similar in macula and the mid peripheral areas (~75%) (Fig. 5J).

Discussion

The data presented are the first demonstration that a calpain-specific cleavage product from α-spectrin (SBDP150) is present in drusen from human retina (Figs. 3B, 5B). The activation of calpain causes accumulation of SBDP in damaged retina and RPE cells. Dysregulated phagocytosis by RPE could cause increased accumulation of calpain-cleaved material in drusen.

Calpains comprise a 15-member family of Ca^{2+}-

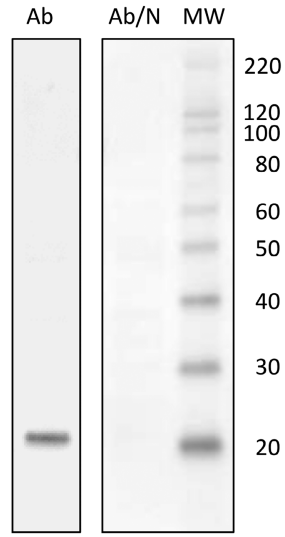

Fig. 4. Recoverin immunoblot and neutralization. Immunoblot of proteins from human normal retina (age 76, Female) showing the expected recoverin band immunostained with recoverin antibody (Ab, 1st lane, left, Mouse polyclonal antibody, Sigma-Aldrich, 1:500). Loss of recoverin band occurred when proteins were treated with recoverin antibody first neutralized with excess human recombinant protein (Ab/N, 2nd lane, full length, Abcam) confirming specificity of antibody and identity of recoverin in Fig. 3F and 5F. MW: markers in kDa (3rd lane).

Table 1. Totals of SBDP150- and recoverin-positive drusen in mid and far periphery, mid periphery, and macula.

A. Counts of drusen positive for recoverin in SBDP150-positive samples.

Group	Nodular drusen in mid and far periphery	Soft drusen in mid periphery*	Nodular drusen in macula	Soft drusen in macula
Normal	1/4	1/1	-	-
Dry AMD	4/6	6/7	1/1	5/7
Wet AMD	1/3	0/3	0/1	1/2
Mixed AMD	2/3	1/2	-	1/3
AMD/Glaucoma	2/5	0/4	-	3/5

B. Summary of drusen totals.

Nodular drusen total	SBDP150+	SBDP150+ & recoverin+	SBDP150+ & recoverin+ / SBDP150+
29	23	11	47.8%
positive drusen%	79.3	37.9	
Soft drusen total	SBDP150+	SBDP150+ & recoverin+	SBDP150+ & recoverin+ / SBDP150+
47	34	18	52.9%
positive drusen%	72.3	38.3	
Drusen total	SBDP150+	SBDP150+ & recoverin+	SBDP150+ & recoverin+ / SBDP150+
76	57	29	50.9%
positive drusen%	75.0	38.2	

A. Totals of drusen separated into groups by nodular and soft drusen location and by AMD group. Nodular drusen are present in the mid and far periphery, while soft drusen are mostly present only in the mid periphery. Counts describe the number of drusen with positive recoverin staining per total number of SBDP150-positive drusen. **B.** Summary of the total drusen numbers and percentage of SBDP150 alone and SBDP150 plus recoverin-positive samples. *Includes two soft drusen that spread across far periphery.

activated cysteine proteases, and are activated by elevated tissue calcium levels in a variety of tissues. In retinal diseases, calpain-dependent proteolysis has been shown to be an underlying mechanism in neuronal degeneration and cell death (Hirata et al., 2015). In our previous study, we found that active calpains 1 and 2 were expressed in normal and AMD donor RPE/choroid samples (Tamada et al., 2007). Calpain 2 showed much higher proteolytic activity than calpain 1 in the RPE/choroid samples from AMD donor eyes. Therefore, we speculate that calpain 2 is the major calpain involved in the accumulation of SBDP150 in drusen. However, since the calcium requirements for full activation of calpain 2 are far higher than for calpain 1, calpain 1 also could be involved in drusen formation.

SBDP150 was detected in both nodular and soft drusen by immunofluorescence. This supports the idea that calpain activity contributed to excess protein accumulation during drusen formation (Figs. 3, 5, 6). Cellular calcium levels increased to a high level (777 ± 64 µM) at 12 hours in human RPE cells fed bovine photoreceptor outer segments (Zhang et al., 2011). Therefore, calcium balance has an important role in phagocytosis and the lipofuscin formation. The major blood protein vitronectin also has a high affinity for Ca^{2+}, enhancing the affinity of vitronectin for hydroxyapatite (HAP). By regulating HAP crystal growth, vitronectin coordinates calcium-phosphate deposition and mineralization of the surface of cholesterol-rich lipids accumulated in the sub-RPE space in AMD (Shin et al., 2020).

During development of drusen, aged RPE cells digest phagocytosed photoreceptor outer segments less efficiently (Inana et al., 2018). This results in accumulation of lipids and cholesterol from photoreceptor outer segments into drusen. This may account for the positive recoverin staining in drusen (Figs. 3F, 5F). These findings support our hypothesis that phagocytosis by RPE increases calcium levels, leading to calpain activation, and accumulation of

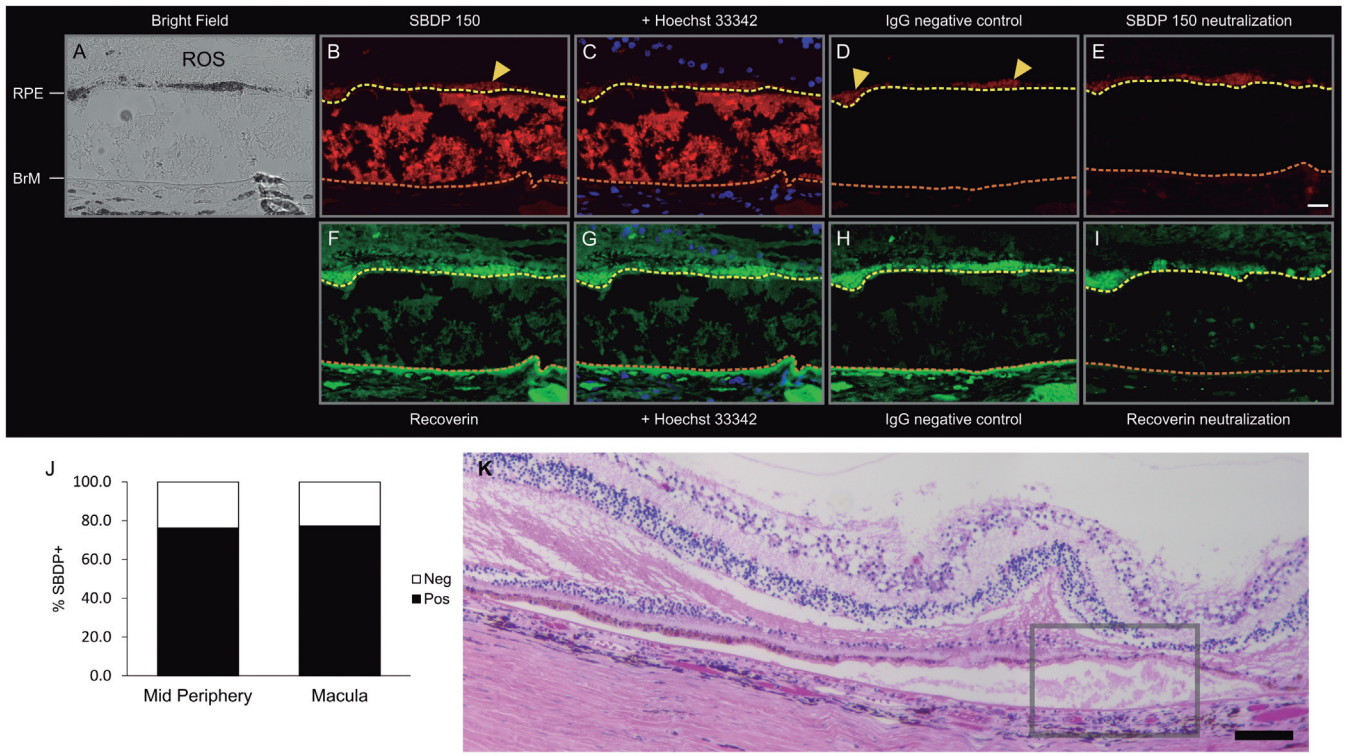

Fig. 5. Immunofluorescence of soft drusen in the macula from a 73-year-old female donor with dry AMD. **A.** Bright field locating the upper area occupied by the rod outer segments (ROS), RPE (upper dark layer), Bruch's membrane (lower transparent line), and separated by a large intervening area of soft drusen. Four consecutive sections were used for same area were observed. **B.** Soft drusen showing strong SBDP150 immunostaining (red). Above the yellow dotted line represents RPE layer and the orange dotted line represents Bruch's membrane. **C.** Counter staining with Hoechst 33342 stain for DNA from cell nuclei (blue) confirmed the location of photoreceptors and outer blood vessel cells (not detected in soft drusen). **D.** Negative IgG control slide showing no SBDP150 staining. However, autofluorescence of the RPE was always present (yellow arrow heads). **E.** Additional negative control showing loss of SBDP150 staining in soft drusen when the slide was treated with neutralized SBDP150 antibody. **F, G.** In place of SBDP150 antibody, soft drusen in this section were processed with an antibody against the photoreceptor protein recoverin, showing positive staining (green) and counter staining with Hoechst 33342 (blue, G). **H.** Negative IgG control slide showing no recoverin staining. **I.** Loss of recoverin staining occurred when the slide was treated with neutralized recoverin antibody. **J.** The percentage of soft drusen positive for SBDP150 was similar in the mid periphery (76.2%, n=21) and in macula (77.3%, n=22) in AMD eyes. **K.** H&E staining with box region of soft drusen at 10x. Scale bars: A-I, 20 μm; K, 100 μm.

calpain-cleaved fragments in drusen. Calpain activation could also act as an important trigger for formation of drusen. Calpain proteolysis is well-known in signaling pathways and is associated with oxidative stress in AMD (Tamada et al., 2007; Nakajima et al., 2017).

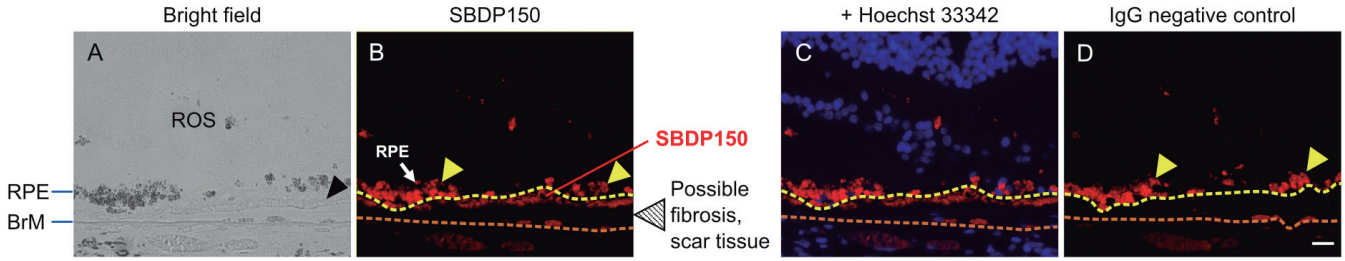

Fig. 6. Immunohistochemistry of soft drusen by SBDP150. Immunohistochemistry of 83 year old male donor with wet AMD, showing positive immunostaining SBDP150 in soft drusen (red). **A.** Bright field showing the upper area occupied by rod outer segments (ROS), RPE (upper dark !ayer), Bruch's membrane (lower transparent line), separated by a large intervening area of soft drusen (black arrowhead). **B.** Soft drusen showing strong red SBDP150 immunostaining. The area above the yellow dotted line is the RPE !ayer. The orange dotted line is Bruch's membrane. **C.** Counter staining with blue Hoechst 33342 for DNA as nuclei marker confirmed the location of photoreceptor and outer blood vessel cells, not detected in soft drusen. **D.** Negative IgG control slide showing lack of SBDP150 staining. However, autofluorescence of the RPE was always present (yellow arrowheads). Scale bar: 20 μm.

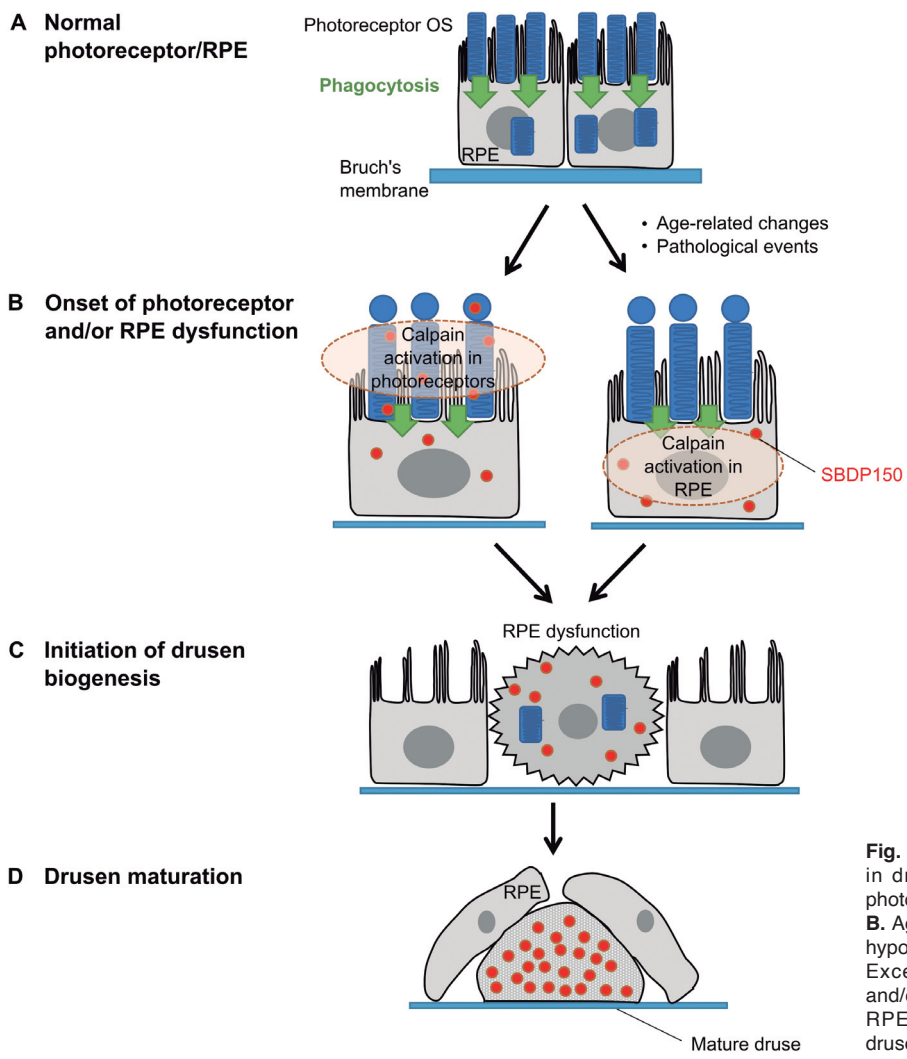

Fig. 7. Hypothesis explaining SBDP150 accumulation in drusen. **A.** Normal phagocytosis of shedding photoreceptor, outer segments in healthy RPE cells. **B.** Age-related changes and pathological events (e.g., hypoxia, oxidative stress) increases localized calcium. Excess calpain activation in photoreceptor cells and/or RPE cells causes SBDP150 accumulation in RPE cells. **C.** Dysfunction of RPE cells triggers drusen biogenesis. **D.** Maturation of drusen.

Calpain and nodular drusen formation during normal aging

Nodular drusen were also observed outside of the macula in aging donors (Lengyel et al., 2004). SBDP150 was found with equal frequency in ~ 80% of the nodular drusen from normal and AMD donors (Fig. 3J). This suggests that drusen formation with SBDP150 accumulation are part of the normal aging process. A step-by-step mechanism for drusen formation is proposed (Fig. 7). Hypoxia or oxidative stress may cause cell damage. Reduced choroidal blood flow has been reported in normal aging eyes (Fig. 7A) (Ardeljan and Chan, 2013). Influx of calcium, calpain activation, and SBDP150 accumulation occurs in photoreceptor and/or RPE cells (Nakajima et al., 2017). RPE cells then phagocytize shed photoreceptor outer segments. This enhances the SBDP150 accumulation in RPE cells. Along with other degradation products-for example; vimentin and vitronectin-leads to dysfunction of RPE cells (Fig. 7B). Drusen biogenesis is triggered by RPE dysfunction allowing RPE-derived components to accumulate in drusen (Spaide et al., 2020). This was demonstrated by finding a photoreceptor marker, recoverin, in drusen (Figs. 3F, 5F, 7C). With time and AMD development, drusen mature. Immune-associated elements, transcription factors, lipid-decorated proteins, and other protein fragments also accumulate during drusen maturation (Curcio, 2018b; Spaide et al., 2020). In addition to α-spectrin, calpains proteolyze numerous other proteins (Ono and Sorimachi, 2012), and such fragments contribute to drusen maturation (Fig. 7D).

Calpain and soft drusen formation in AMD

Large soft drusen are characteristic of AMD where they cause loss of central vision (Curcio, 2018a). Soft drusen lead to serous RPE detachment, choroidal neovascularization, and disciform scarring (Gheorghe et al., 2015). Acceleration of the calpain activation process could be associated with increasing drusen size-a hallmark of AMD. Confluent drusen would result in further ischemia due to thickening of RPE/BrM. Retina and RPE cell detachment also reduce oxygen influx from the choroid (Tisi et al., 2021). Our data suggest that acceleration of calpain-induced proteolysis contributes to the production of soft drusen in AMD.

Approximately 25% of soft drusen in the AMD donors did not show SBDP150 signal (Fig. 5J). Some of them were big enough to spread across from mid to far periphery. Reasons for this finding include: 1) SBDP150 levels were lower than the detection limit of immunofluorescence. 2) SBDP150 was further degraded to smaller, non-immunogenic fragments. Severe degradation has been observed in cultured monkey RPE cells (Nakajima et al., 2017). 3) Maturation of some drusen could have been completed before calpain activation occurred in retina. When nodular drusen were smaller than approximately 63 µm (Friberg et al., 2012), they were negative for SBDP150 (Fig. 8). In contrast, larger drusen were positive for SBDP150.

Our recoverin data support the evidence that photoreceptor proteins are found in some drusen. But signal strength for recoverin varied. Some drusen were negative, while other drusen showed positive signals for recoverin that varied from weak to dense. Un-esterified

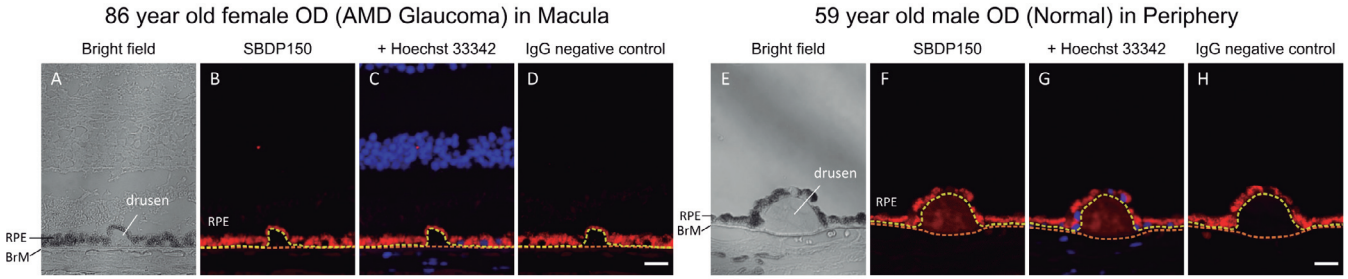

I. Nodular drusen size and SBDP150 staining

	Mid and Far Periphery			Macula		
	Drusen Size			Drusen Size		
	<63 µM	63–124 µM	>124 µM	<63 µM	63–124 µM	>124 µM
Nodular drusen total	28	21	1	3	2	0
SBDP150+	16	20	1	0	2	0
positive drusen %	57.1	95.2	100.0	0.0	100.0	-

Fig. 8. Immunohistochemistry of nodular drusen by SBDP150. Immunohistochemistry of nodular drusen in the macula from an 86 year old female donor with AMD and glaucoma **(A-D)** and from a normal 59 year old male donor **(E-H)**. **A, E.** Bright field locating RPE (upper dark !ayer), Bruch's membrane (lower transparent line). **B, F.** Nodular drusen showing SBDP150 immunostaining (red). Area above the yellow dotted line represents the RPE !ayer and the orange dotted line represents Is Bruch's membrane. **C, G.** Counter staining with Hoechst 33342 stain for DNA from cell nuclei (blue). **D, H.** Negative IgG control slide showing lack of SBDP150 staining. **I.** Staining frequency of SBDP150 in the periphery and lateral areas was related to drusen diameter: <63 µm=57.1%, while 63-124 µm=95.2%, and >124 µm=100%. Scale bar: 20 μm.

cholesterol, a component of outer segment membranes was more concentrated in drusen than in outer segments (Curcio et al., 2005). These data support the idea that photoreceptors phagocytosed by RPE cells were delivered to drusen. However, other reports show that photoreceptor components, such as interphotoreceptor matrix-1, chondroitin sulfate proteoglycan, opsin (Kamao et al., 2014), and RPE marker protein RPE65 (data not shown) were negative in drusen. Protein signal variations between drusen may be dependent on the timing between degradation of photoreceptor components in RPE and formation of each particular druse.

To our knowledge, the proteomics studies on postmortem human drusen did not detect proteases (Lambert et al., 2016). Our study is based on a relatively small number of 22 pathologic eyes. Further investigation with a larger number of samples with a wider range of AMD would help confirm our results. Proteomics on punches centered on the macula and mid peripheral areas to discover specific calpain cleavage sites on other proteins would be useful for localizing calpain activity.

Preventing AMD progression is important for protection of visual function. AREDS2 antioxidants-vitamin C and E, lutein, zeaxanthin, zinc and copper-were effective in slowing progression of AMD (Age-Related Eye Disease Study 2 (AREDS2) Research Group, et al., 2014). A number of candidate medicines are also under investigation (Bahadorani and Singer, 2017). A complement C3 inhibitor, pegcetacoplan, was recently approved for treatment of geographic atrophy, a condition where the non-exudative area is larger than RPE atrophy. The current study was the first to detect signatures of calpain activation in drusen from AMD donor eyes. Further molecular studies are needed to prove that calpain-induced proteolysis participates in the degeneration of photoreceptor and RPE cells in AMD. Calpain inhibitors, such as SNJ-1945 (Hirata et al., 2015), may inhibit the degradation of photoreceptor and/or RPE cells in AMD.

Acknowledgements. We gratefully thank Dr. Daniel Albert and Dr. Hillary Stiefel (Casey Eye Institute, Oregon Health Science & University) for help in distinguishing soft drusen. The potential conflict of interests for Thomas R. Shearer, Mitsuyoshi Azuma, Emi Nakajima, Momoko Kobayashi-Otsugu and Kana Orihara were reviewed, and a management plan approved by the OHSU Conflict of Interest in Research Committee was implemented. The research of this work was funded by Senju Pharmaceutical Co., Ltd.

Author's Contribution. MA, MK and EN designed the experiments. TS and MA supervised the project, the main conceptual ideas and proof outline. KO and MK performed the experiments and the analysis of the results with EN's support. RW contributed the image formatting for the manuscript. DW contributed to the interpretation and analysis of the results and to the writing of the manuscript. TS and MA provided critical feedback and helped shape the research, analysis and manuscript. KO, MK, EN, RW, TS and MA wrote and revised the manuscript.

References

Age-Related Eye Disease Study 2 (AREDS2) Research Group, Chew E.Y., Clemons T.E., Sangiovanni J.P., Danis R.P., Ferris F.L. 3rd, Elman M.J., Antoszyk A.N., Ruby A.J., Orth D., Bressler S.B., Fish G.E., Hubbard G.B., Klein M.L., Chandra S.R., Blodi B.A., Domalpally A., Friberg T., Wong W.T., Rosenfeld P.J., Agrón E., Toth C.A., Bernstein P.S. and Sperduto R.D. (2014). Secondary analyses of the effects of lutein/zeaxanthin on age-related macular degeneration progression: AREDS2 report No. 3. JAMA Ophthalmol. 132, 142-149.

Ardeljan D. and Chan C.C. (2013). Aging is not a disease: distinguishing age-related macular degeneration from aging. Prog. Retin. Eye Res. 37, 68-89.

Azuma M., Chung K., Fujii A. and Shearer T.R. (2010). Patient selection criteria for pilot studies on amelioration of non-neovascular age-related macular degeneration. J. Ocul. Pharmacol. Ther. 26, 367-371.

Bahadorani S. and Singer M. (2017). Recent advances in the management and understanding of macular degeneration. F1000Res. 6, 519.

Bermond K., Berlin A., Tarau I.S., Wobbe C., Heintzmann R., Curcio C.A., Sloan K.R. and Ach T. (2021). Characteristics of normal human retinal pigment epithelium cells with extremes of auto-fluorescence or intracellular granule count. Ann. Eye Sci. 6, 3.

Chakravarthy U., Wong T.Y., Fletcher A., Piault E., Evans C., Zlateva G., Buggage R., Pleil A. and Mitchell P. (2010). Clinical risk factors for age-related macular degeneration: a systematic review and meta-analysis. BMC Ophthalmol. 10, 31.

Curcio C.A. (2018a). Soft drusen in age-related macular degeneration: biology and targeting, via the Oil Spill Strategy. Invest. Ophthalmol. Vis. Sci. 59, AMD160-AMD181.

Curcio C.A. (2018b). Antecedents of soft drusen, the specific deposit of age-related macular degeneration, in the biology of human macula. Invest. Ophthalmol. Vis. Sci. 59, AMD182-AMD194.

Curcio C.A., Presley J.B., Malek G., Medeiros N.E., Avery D.V. and Kruth H.S. (2005). Esterified and unesterified cholesterol in drusen and basal deposits of eyes with age-related maculopathy. Exp. Eye Res. 81, 731-741.

Fernandez-Godino R., Pierce E.A. and Garland D.L. (2016). Extracellular matrix alterations and deposit formation in AMD. Adv. Exp. Med. Biol. 854, 53-58.

Friberg T.R., Bilonick R.A. and Brennen P. (2012). Is drusen area really so important? An assessment of risk of conversion to neovascular AMD based on computerized measurements of drusen. Invest. Ophthalmol. Vis. Sci. 53, 1742-1751.

Gambril J.A., Sloan K.R., Swain T.A., Huisingh C., Zarubina A.V., Messinger J.D., Ach T. and Curcio C.A. (2019). Quantifying retinal pigment epithelium dysmorphia and loss of histologic autofluorescence in age-related macular degeneration. Invest. Ophthalmol. Vis. Sci. 60, 2481-2493.

Gheorghe A., Mahdi L. and Musat O. (2015). Age-related macular degeneration. Rom. J. Ophthalmol. 59, 74-77.

Hendrickson A., Bumsted-O'Brien K., Natoli R., Ramamurthy V., Possin D. and Provis J. (2008). Rod photoreceptor differentiation in fetal and infant human retina. Exp. Eye Res. 87, 415-426.

Hirata M., Shearer T.R. and Azuma M. (2015). Hypoxia activates calpains in the nerve fiber layer of monkey retinal explants. Invest. Ophthalmol. Vis. Sci. 56, 6049-6057.

Inana G., Murat C., An W., Yao X., Harris I.R. and Cao J. (2018) RPE phagocytic function declines in age-related macular degeneration and is rescued by human umbilical tissue derived cells. J. Transl. Med. 16, 63.

Kamao H., Mandai M., Okamoto S., Sakai N., Suga A., Sugita S., Kiryu J. and Takahashi M. (2014). Characterization of human induced pluripotent stem cell-derived retinal pigment epithelium cell sheets aiming for clinical application. Stem Cell Rep. 2, 205-218.

Lambert N.G., ElShelmani H., Singh M.K., Mansergh F.C., Wride M.A., Padilla M., Keegan D., Hogg R.E. and Ambati B.K. (2016). Risk factors and biomarkers of age-related macular degeneration. Prog. Retin. Eye Res. 54, 64-102.

Lengyel I., Tufail A., Hosaini H.A., Luthert P., Bird A.C. and Jeffery G. (2004) Association of drusen deposition with choroidal intercapillary pillars in the aging human eye. Invest. Ophthalmol. Vis. Sci. 45, 2886-28892.

Nakajima E., Hammond K.B., Rosales J.L., Shearer T.R. and Azuma M. (2011) Calpain, not caspase, is the causative protease for hypoxic damage in cultured monkey retinal cells. Invest. Ophthalmol. Vis. Sci. 52, 7059-7067.

Nakajima E., Hammond K.B., Hirata M., Shearer T.R. and Azuma M. (2017). Contribution of calpain and caspases to cell death in cultured monkey RPE cells. Invest. Ophthalmol. Vis. Sci. 58, 5412-5420.

Ono Y. and Sorimachi H. (2012). Calpains: An elaborate proteolytic system. Biochim. Biophys. Acta 1824, 224-236.

Quinn N., Csincsik L., Flynn E., Curcio C.A., Kiss S., Sadda S.R., Hogg R., Peto T. and Lengyel I. (2019). The clinical relevance of visualising the peripheral retina. Prog. Retin. Eye Res. 68, 83-109.

Shin K., Kent J.E., Singh C., Fujimoto L.M., Yu J., Tian Y., Im W. and Marassi F.M. (2020). Calcium and hydroxyapatite binding site of human vitronectin provides insights to abnormal deposit formation. Proc. Natl. Acad. Sci. USA 117, 18504-18510.

Spaide R.F., Jaffe G.J., Sarraf D., Freund K.B., Sadda S.R., Staurenghi G., Waheed N.K., Chakravarthy U., Rosenfeld P.J., Holz F.G., Souied E.H., Cohen S.Y., Querques G., Ohno-Matsui K., Boyer D., Gaudric A., Blodi B., Baumal C.R., Li X., Coscas G.J., Brucker A., Singerman L., Luthert P., Schmitz-Valckenberg S., Schmidt-Erfurth U., Grossniklaus H.E., Wilson D.J., Guymer R., Yannuzzi L.A., Chew E.Y., Csaky K., Monés J.M., Pauleikhoff D., Tadayoni R. and Fujimoto J. (2020). Consensus nomenclature for reporting neovascular age-related macular degeneration data: Consensus on neovascular age-related macular degeneration nomenclature study Group. Ophthalmology 127, 616-636.

Sura A.A., Chen L., Messinger J.D., Swain T.A., McGwin G. Jr, Freund K.B. and Curcio C.A. (2020). Measuring the Contributions of Basal Laminar Deposit and Bruch's Membrane in Age-Related Macular Degeneration. Invest. Ophthalmol. Vis. Sci. 61, 19.

Tamada Y., Walkup R.D., Shearer T.R. and Azuma M. (2007). Contribution of calpain to cellular damage in human retinal pigment epithelial cells cultured with zinc chelator. Curr. Eye Res. 32, 565-573.

Tisi A., Feligioni M., Passacantando M., Ciancaglini M. and Maccarone R. (2021). The impact of oxidative stress on blood-retinal barrier physiology in age-related macular degeneration. Cells 10, 64.

Yang S., Zhao J. and Sun X. (2016). Resistance to anti-VEGF therapy in neovascular age-related macular degeneration: a comprehensive review. Drug Des. Devel. Ther. 10, 1857-1867.

Zhang L., Hui Y.N., Wang Y.S., Ma J.X., Wang J.B. and Ma L.N. (2011). Calcium overload is associated with lipofuscin formation in human retinal pigment epithelial cells fed with photoreceptor outer segments. Eye (Lond) 25, 519-527.

Accepted June 1, 2023